Neoplasma 2024; 71(3): 219–230

doi:10.4149/neo_2024_230616N316

Silencing of lncRNA LOC105376794 promotes migration, invasion, and gefitinib resistance of lung adenocarcinoma cells with EGFR 19del mutation by ATF4/CHOP axis and ERK phosphorylation

Wenjing LIU[1], Zhipeng DUAN[2], Yefeng WU[3], Rui MA[1,*]

[1]Medical Oncology Department of Thoracic Cancer (2), Cancer Hospital of China Medical University, Cancer Hospital of Dalian University of Technology, Liaoning Cancer Hospital and Institute, Shenyang, Liaoning, China; [2]Department of Gastrointestinal Surgery, Shenyang Anorectal Hospital, Shenyang, Liaoning, China; [3]Central Laboratory, Cancer Hospital of China Medical University, Cancer Hospital of Dalian University of Technology, Liaoning Cancer Hospital and Institute, Shenyang, Liaoning, China

**Correspondence: marui@cancerhosp-ln-cmu.com*

Received June 16, 2023 / Accepted May 30, 2024

Epidermal growth factor receptor (EGFR) gene exon 19 in-frame deletion (19del) and exon 21 L858R point mutation (21L858R mutation) are prevalent mutations in lung adenocarcinoma. Lung adenocarcinoma patients with 19del presented with a better prognosis than the 21L858R mutation under the same epidermal growth factor receptor tyrosine kinase inhibitor treatment. Our study aimed to uncover the expression of long non-coding RNA LOC105376794 between 19del and 21L858R mutation, and explore the mechanism that regulates cells' biological behavior and gefitinib sensitivity in lung adenocarcinoma cells with 19del. Transcriptome sequencing was conducted to identify differentially expressed lncRNAs between EGFR 19del and 21L858R mutation in serum through the DNBSEQ Platform. Protein-protein interaction network and Kyoto Encyclopedia of Genes and Genomes pathway were conducted to analyze the relationship between lncRNAs and mRNAs through STRING and Dr. TOM. Reverse transcription-quantitative polymerase chain reaction (RT-qPCR) was used to measure the expression of lncRNA LOC105376794 in serum and cells. Loss-of-function experiments were used to validate the biological function and gefitinib sensitivity of LOC105376794 in lung adenocarcinoma cells. Protein levels were detected by western blotting. Through transcriptome resequencing and RT-qPCR, we found the expression levels of LOC105376794 in serum were increased in the 19del group compared with the 21L858R mutation group. Inhibition of LOC105376794 promoted proliferation, migration and invasion, and reduced apoptosis of HCC827 and PC-9 cells. The low expression of LOC105376794 reduced gefitinib sensitivity in PC-9 cells. Mechanistically, we found that the knockdown of LOC105376794 suppressed activating transcription factor 4 (ATF4)/C/EBP homologous protein (CHOP) signaling pathway and facilitated the expression of extracellular signal-regulated kinase 1/2 (ERK) phosphorylation. LOC105376794 altered cell biological behavior and gefitinib sensitivity of lung adenocarcinoma cells with 19del through the ATF4/CHOP signaling pathway and the expression of ERK phosphorylation. The results further illustrated the fact that lung adenocarcinoma patients with 19del presented with a more favorable clinical outcome and provided a theoretical basis for treatment strategy for lung adenocarcinoma patients with 19del.

Key words: lung adenocarcinoma; lncRNA LOC105376794; EGFR gene exon 19 in frame deletion; gefitinib resistance; ATF4/CHOP; ERK phosphorylation

Epidermal growth factor receptor (EGFR) gene exon 19 in-frame deletion (19del) and exon 21 L858R point mutation (21L858R mutation) are prevalent mutations in lung adenocarcinoma (LUAD), accounting for approximately 85% of EGFR mutations [1]. Existing evidence has validated the functionality of 19del and 21L858R mutation as predictive indicators of epidermal growth factor receptor tyrosine kinase inhibitors (EGFR-TKIs) in advanced LUAD [2]. However, LUAD patients with 19del and 21L858R mutation presented with different outcomes under the same EGFR-TKI treatment. Clinical reports have indicated that LUAD patients with 19del had better survival than 21L858R mutation [3–5]. Theoretically, many factors contribute to the distinct prognosis. For example, a mutation of the EGFR kinase domain modified its own structure and facilitated abnormal activation of EGFR and downstream kinase, thus

inducing anti-apoptosis or proliferation in cancer cells [6]. Furthermore, the variable outcomes are consequent of the copy numbers of EGFR genes [7], binding abilities between EGFR mutation locus and EGFR-TKIs [8, 9], tumor mutation burden [10, 11], and combination of rare mutations [12], or co-mutation in the same tumor [13]. Currently, insight into discrepant clinical prognosis between 19del and 21L858R mutation remains elusive.

Transcriptome sequencing is a comprehensive procedure for differential expression and biological function analysis of RNA molecules [14], providing a vital foundation for the underlying molecular mechanism in disease development. The identification of differentially expressed genes with biological functions can not only seek biomarkers for EGFR mutation status as supplementary but also contribute to explaining the different consequences of clinical studies based on 19del and 21L858R mutation. Long non-coding RNAs (lncRNAs), critical for the pattern of gene expression at transcriptional as well as post-transcriptional levels, have elicited involvement in various physiological processes [15, 16]. lncRNA LOC105376794 is located on chromosome 1 with a length of 10,943 nt. Gene Cards shows that LOC105376794 mRNA is expressed in many normal tissues, such as the immune system, nervous system, digestive system, respiratory system, and so on. LOC105376794 combines with a variety of promoters and enhancers in order to mediate target genes. Whereas, the mechanism of LOC105376794 regulating LUAD cells with 19del has not been explored.

For this article, we investigated the differential expression of LOC105376794 in LUAD patients and cells between 19del and 21L858R mutation. The study intended to inquire into the biofunction and regulatory mechanism in gefitinib sensitivity of LOC105376794 in LUAD cells with 19del.

Patients and methods

Sample collection and preparation. The study was conducted according to the guidelines of the Declaration of Helsinki, and approved by the Institutional Review Board of Liaoning Cancer Hospital (20220318G, March 18th, 2022). All patients gave informed consent.

Prior to TKI treatment, peripheral blood (2 ml) was withdrawn respectively from 3 LUAD patients with 21L858R and 3 patients with 19del. Fresh blood was placed at room temperature for 20–60 min. The coagulated samples were centrifuged at 4 °C 1,600×g. The supernatant was recentrifuged at 4 °C 16,000×g. The remaining supernatant was preserved at –80 °C. EGFR mutation status was performed by quantitative real-time PCR (qRT-PCR) or next-generation sequencing.

Serum RNA extraction and transcriptome sequencing. Total RNA content was obtained from the serum sample. The Agilent 2100 Bioanalyzer was utilized for RNA molecular weight determination, quantitative analysis, and quality control. The RNA contents of six samples were consistent with the requirements for quality inspection. Transcriptome sequencing was conducted using the DNBSEQ Platform (The Beijing Genomics Institute, China). The purified process for the total RNA content was the removal of rRNA from total RNA & fragment, the addition of dNTP and first strand synthesis, the addition of dUTP and second strand synthesis (dTTP-dUTP), the addition of 'A' and adapter, PCR amplification, single-strand formation, and cyclization. The raw reads from sequencing were processed to remove rRNA, low-quality reads, and reads with contamination to help to improve the credibility of the results. Next, the purified reads were aligned with the reference genome (Homo_sapiens, NCBI, GCF_000001405.39_GRCh38.p13) and the transcriptome by HISAT [17] (Hierarchical Indexing for Spliced Alignment of Transcripts) for subsequent analysis. Each sample produced an average of 10.69 g data.

Reverse transcription quantitative polymerase chain reaction (RT-qPCR). Total RNA was extracted from cell lines and serum using RNAiso Plus (Takara, Dalian, China) and reverse transcribed to cDNA with a Reverse Transcription Kit (Takara). The expressions of lncRNAs were measured by SYBR Premix Ex Taq kit (Takara) on a Step One Plus Real Time-PCR System with a protocol of 95 °C for 5 min, then amplification with 40 cycles at 95 °C for 15 s, at 60 °C for 20 s, and finally at 72 °C for 40 s. The relative expression of serum LOC105376794 was analyzed by the $2^{-\Delta Ct}$ method using β-actin as the reference gene. The relative expressions of LOC105376794 in cells were calculated by the $2^{-\Delta\Delta Ct}$ method using GAPDH as an internal control. The sequences of primers were as described below: β-actin: F: ATGTGGCCGAGGACTTTGATT, R: AGTGGGGTGGCTTTTAGGATG. GAPDH: F: AGATCATCAGCAATGCCTCCT, R: TGAGTCCTTCCACGATACCAA. LOC105376794: F: GCTGAAAGGCCACATCTCAC, R: CGATTCCTCCCCACAATCCT.

Cell lines and culture. Lung adenocarcinoma cell lines HCC827 and PC-9 were with EGFR 19del, and NCI-H1975 cells were with EGFR 21L858R mutation. HCC-827 cell line was purchased from the National Collection of Authenticated Cell Cultures (Shanghai, China) and PC-9 cell line was purchased from iCell Bioscience Inc (Shanghai, China). NCI-H1975 cell line was from the National Collection of Authenticated Cell Cultures (Shanghai, China). All cells were incubated at 37 °C in a DMEM mixture with 10% fetal bovine serum and 5% carbon dioxide atmosphere.

Construction of plasmids and cell transfection. Short harpin RNAs (sh-RNAs) for LOC105376794 (LOC105376794-RNAi #8422: 5'-GATCCCGCTCCCTGAGCACAATTTATTCTCGAGAATAAATTGTGCTCAGGGAGCTTTTTGGAT-3', LOC105376794-RNAi #8423: 5'-GATCCCGAGGAATCGGCGTAGAGATGACTCGAGTCATCTCTACGCCGATTCCTCTTTTTGGAT-3', LOC105376794-RNAi #8424: 5'-GATCCCGCTGAAAGGCCACATCTCACTCTCGAGAGTGAGATGTGGCCTTTCAGCTTTTTGGAT-3') and the negative

control (sh-NC: 5'-GATCCCTTCTCCGAACGTGTCAC-GTTTTTTGGAT-3') were constructed by GeneChem (Shanghai, China). Following the instructions, all plasmid transfection was performed for 48 h using Lipofectamine 3000 according to the instructions (Invitrogen, USA).

Colony formation and cell counting kit-8 (CCK-8) assays. The proliferative abilities of cells were using a CCK-8 assay (KeyGen Bio TECH, Jiangsu, China). Transfected cells were spread (4×10^4/ml) into a 96-well plate. CCK-8 reagent (10 μl) was added to each well to each well at day 0, 1, 2, and 3. After incubation for 2 h at 37 °C, the absorbance values were measured at 450 nm using a microplate reader (BioTek, USA).

Cell apoptosis assay. An Annexin-V APC/7-AAD apoptosis kit (KeyGen Bio TECH, Jiangsu, China) was used to assess cell apoptosis and the apoptosis rate of cells under gefitinib treatments. Cells were collected and incubated in the dark for 15 min with Annexin V-APC (5 μl) and 7-AAD (5 μl), then measured by a flow cytometer (BECKMAN COULTER CytoFLEX, USA). Cisplatin-treated cells were used for cytometer setup and apoptosis control.

Cell migration and invasion assays. Cell invasion and migration tests were examined by Transwell assays and wound healing. Transwell chamber (#3422, Corning Incorporated, USA) and Matrigel Invasion Chamber (#356234, BD, USA) were used in Transwell assays. Transfected cells (1×10^5/ml) were seeded into the upper chamber. A complete medium (including 20% FBS) was added to the lower chamber to induce cell invasion. After incubation for 24 h, membranes were fixed, immersed in 1% crystal violet, and photographed using an inverted microscope (OLYMPUS, Japan) to enumerate cells. For the wound-healing assay, cells (6×10^4/well) were added into 6-well plates, and a 100 μl pipette tip was used to create a wound. After incubation for 24 h with serum-free medium, the distance was imaged with an inverted microscope (OLYMPUS, Japan).

Western blotting. Total protein was extracted from cells using a RIPA lysis buffer (KeyGen Bio TECH, Jiangsu, China). Protein concentrations were examined using a bicinchoninic acid protein assay kit (KeyGen Bio TECH, Jiangsu, China). The proteins were separated by 10% SDS polyacrylamide gel electrophoresis (Beyotime, China) and transferred to the nitrocellulose filter membrane. Subsequently, the membranes were blocked with 5% non-fat milk for 2 h and then were incubated with primary antibodies at 4 °C overnight. After washing, the membranes were incubated with secondary antibodies (anti-mouse IgG or anti-rabbit IgG) at room temperature for 2 h. Finally, the membranes were detected and visualized with an enhanced chemiluminescence system (SYNGENE, UK). The primary antibodies are as follows: ERK (Abcam, ab17942, anti-rabbit IgG, 1:1000), p-ERK (Abcam, ab201015, anti-rabbit IgG, 1:1000), ATF4 (Immunoway, YT1102, anti-rabbit IgG, 1:1000), CHOP (Immunoway, YT0912, anti-rabbit IgG, 1:1000), anti-cleaved caspase-3 (Abcam, ab32042, anti-rabbit IgG, 1:1000), pro-caspase-3 (Proteintech, 19677-1-ap, anti-rabbit IgG, 1:1000), β-actin (Immunoway, YM3028, anti-mouse IgG, 1:3000), GAPDH (Abcam, ab8245, anti-mouse IgG, 1:1000). The amount of loaded protein was 15 μg, such as ATF4, CHOP, ERK, p-ERK, and the duration of signal acquisition time was 1–2 min with ECL kit (KGC4601, KeyGen Bio TECH, China). The amounts of cleaved caspase-3 and pro-caspase-3 loaded protein were 15 μg, and the duration of signal acquisition time was 21 s with New-SUPER ECL kit (KGC4602-200, KeyGen Bio TECH, China). We used ChemiDoc MP Imaging System (Bio-Rad, USA) to capture the images of protein bands and Gel-Pro32 software quantitatively to analyze the protein bands.

Statistical analysis. SPSS 18.0 was performed for statistical analyses. We repeated the experiment three times. Fisher's exact test or Pearson's χ^2 test was used for the comparison of categorical variable differences. Paired t-test was to analyze paired data in two groups. Spearman correlation was conducted for correlation analysis. A p-value <0.05 was considered to be statistically significant. Differentiated expressed genes were identified using the Dr. TOM platform, a data mining system of BGI. Clean reads were aligned with the reference sequence using Bowtie [18], and the expression patterns of genes were normalized and calculated using RSEM [19]. DESeq2 [20] was adopted to determine the expression patterns of altered genes in each sample, Qvalue (Adjusted p-value) ≤0.05. The differentially expressed genes were represented as log2FC, which meant log-transformed fold change (log2FC = log2[L858R] – log2[19del]. Protein-protein interaction network and Kyoto Encyclopedia of Genes and Genomes pathway were analyzed in STRING and Dr. TOM. The protein-protein interaction and Kyoto Encyclopedia of Genes and Genomes terms with corrected $p\leq0.05$ were considered to be significant and were further to view the interconnected categories using Cytoscape [21].

Results

Expression and pathways analysis of differentially expressed lncRNAs. A total of 356 differentially expressed lncRNAs were identified, of which 202 were overexpressed in the 21L858R mutation group and 154 lncRNAs were upregulated in the 19del group. In network analysis, 54 differentially expressed lncRNAs evidently interacted with mRNAs (rnaplex max MFE = –100, max num = 10) (Figure 1, Supplementary Figure S1, Supplementary Figure S2). Among them, 31 lncRNAs were elevated in 19del, interacting with 94 mRNAs (Supplementary Table S1). These lncRNAs could potentially be involved in lipoic acid metabolism, RAP1A signaling pathway, cell cycle, and so on (Supplementary data S1). Among the lncRNAs elevated in 19del, there were 10 lncRNAs upregulated in the 19del group that interacted with more than 3 mRNAs (Figure 1). Meanwhile, 23 lncRNAs were upregulated in 21L858R mutation (Supplementary Table S1), interacting with 59 mRNAs (Supplementary Figure S2), and could participate in Fatty acid biosynthesis,

Calcium signaling pathway, cyclic guanosine monophosphate (GMP)-protein kinase G (PKG) signaling pathway, and so on. In positional analysis, 10 lncRNAs evidently interacted with mRNAs (Qvalue <0.05 and |log2FC| ≥2) (Supplementary data S2). Among them, 4 lncRNAs (PCNA-AS1, LOC100130744, LOC101929243, SH3BP5-AS1) elevated in 19del were associated with 4 mRNAs and may be involved in nucleotide excision repair, base excision repair, DNA replication, and so on (Supplementary data S2). Meanwhile, 6 lncRNAs (PDCD6-AHRR, BGIG9606_100340, ATP1A1-AS1, PSMB8-AS1, BGIG9606_100325, TGFB2-OT1) upregulated in 21L858R mutation were associated with 6 mRNAs (Supplementary data S2) and could participate in the cGMP-PKG signaling pathway, mitogen-activated protein kinases signaling pathway, Proteasome, and so on.

LncRNA LOC105376794 is upregulated in the 19del group of lung adenocarcinoma. There were 56 patients' sera with advanced LUAD enrolled in this study, including 21 cases with 19del, 21 cases with 21L858R mutation, and 14 cases with EGFR wild-type. The patients with 19del and 21L858R mutation received first-line EGFR-TKIs treatment. The patients' characteristics are listed in Table 1. We analyzed lncRNA LOC105376794 expression in LUAD serum. The results in Figure 2A indicated that the expression levels of serum LOC105376794 were significantly decreased in the EGFR 19del and 21L858R group in comparison to the EGFR wild-type group. There was no differential expression of LOC105376794 by sex and smoking stratification in all the patients (Table 2). The expression level of serum LOC105376794 was dramatically upregulated in the 19del group compared with the 21L858R mutation group (Figure 2A). LOC105376794 expression in serum showed a positive correlation tendency with PFS in the 21L858R mutant group, but the result did not reach significance (Spearman correlation coefficient = 0.41, p=0.21). The levels of LOC105376794 in HCC827 and PC-9 cells were considerably upregulated in comparison to H1975 cells (Figure 2B).

Inhibition of lncRNA LOC105376794 promotes proliferation and reduces apoptosis of HCC827 and PC-9 cells. We carried out loss-of-function investigations in

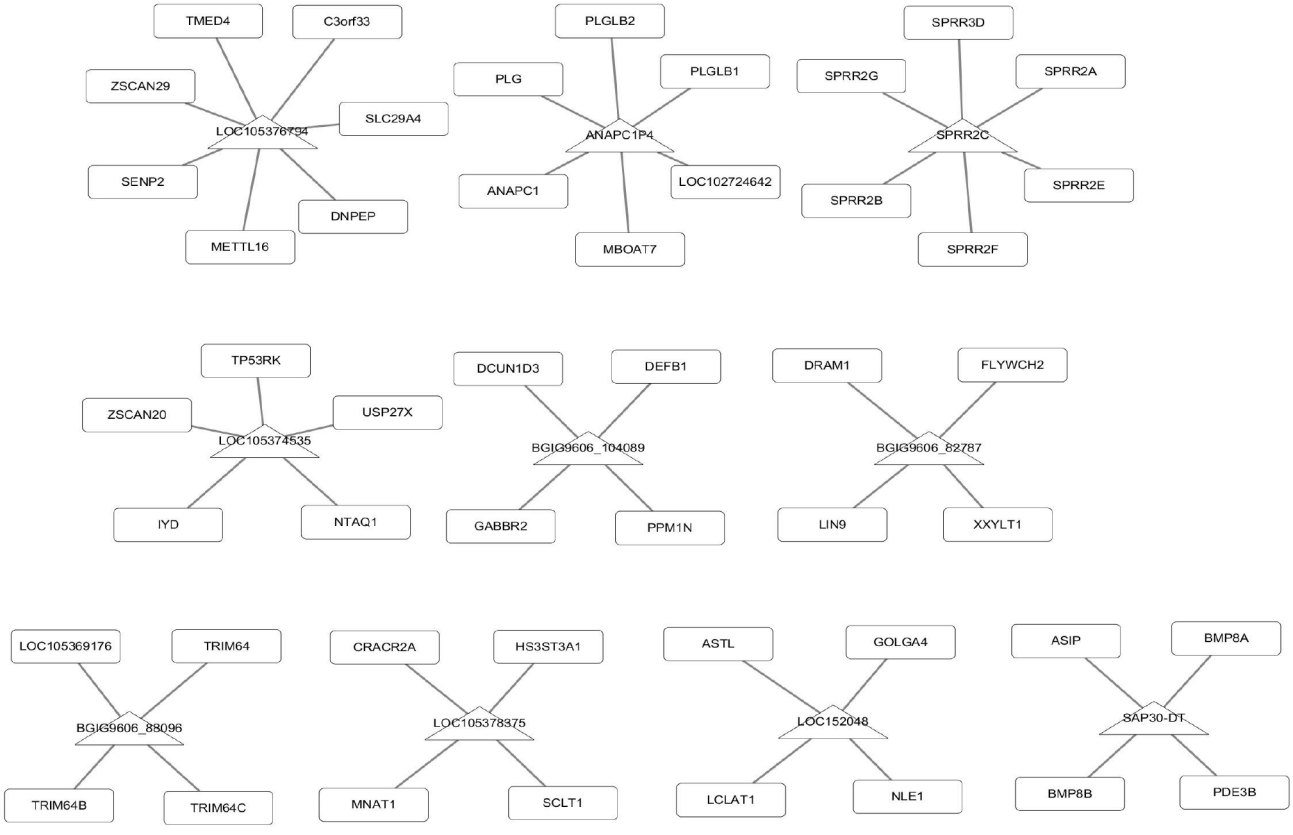

Figure 1. The lncRNAs upregulated in the 19del group interacted with more than 3 mRNAs. There were 10 lncRNAs upregulated in the 19del group that interacted with more than 3 mRNAs. The triangles mean lncRNAs upregulated in the 19del group, and the ovals mean the interacting mRNAs. These mRNAs were ANAPC1, ASIP, ASTL, BMP8A, BMP8B, C3orf33, CRACR2A, DCUN1D3, DEFB1, DNPEP, DRAM1, FLYWCH2, GABBR2, GOLGA4, HS3ST3A1, IYD, LCLAT1, LIN9, LOC102724642, LOC105369176, MBOAT7, METTL16, MNAT1, NLE1, NTAQ1, PDE3B, PLG, PLGLB1, PLGLB2, PPM1N, SCLT1, SENP2, SLC29A4, SPRR2A, SPRR2B, SPRR2E, SPRR2F, SPRR2G, SPRR3D, TMED4, TP53RK, TRIM64, TRIM64B, TRIM64C, USP27X, XXYLT1, ZSCAN20, and ZSCAN29.

Table 1. Clinical characteristics of LUAD patients.

Clinical characteristics	19del & 21L858R mutation vs. EGFR wild-type group		p-value	Clinical characteristics	19del vs. 21L858R mutation		p-value
	19del & 21L858R mutation (n=42)	EGFR wild-type group (n=14)			19del (n=21)	21L858R mutation (n=21)	
Sex			0.03	Sex			0.32
male	13 (31.0%)	9 (64.3%)		male	8 (38.1%)	5 (23.8%)	
female	29 (69.0%)	5 (35.7%)		female	13 (61.9%)	16 (76.2%)	
Age			0.88	Age			0.76
≤58	23 (54.8%)	8 (57.1%)		≤ 58	12 (57.1%)	11 (52.4%)	
>58	19 (45.2%)	6 (42.9%)		> 58	9 (42.9%)	10 (47.6%)	
Smoking status			0.01	Smoking status			0.66
never smoker	36 (85.7%)	7 (50.0%)		never smoker	17 (81.0%)	18 (85.7%)	
ever smoker	6 (14.3%)	7 (50.0%)		ever smoker	4 (19.0%)	3 (14.3%)	
Drinking status			1	Drinking status			1
never drinker	39 (92.9%)	13 (92.9%)		never drinker	19 (90.5%)	19 (90.5%)	
ever drinker	2 (7.1%)	1 (7.1%)		ever drinker	2 (9.5%)	2 (9.5%)	

HCC827 and PC-9 cells with relatively high expression of LOC105376794. HCC827 and PC-9 cells were transfected with sh-LOC105376794 to construct a knockdown model, which was confirmed by qRT-PCR. In Figure 2C, the expression of LOC105376794 was significantly decreased after transfection with sh-LOC105376794 (LOC105376794-RNAi #8424). The CCK-8 assay showed that the proliferation of HCC827 and PC-9 cells was increased by the knockdown of LOC105376794 after 72 h (Figure 3A).

Cell apoptosis assay showed the reduction of LOC105376794 expression in HCC827 and PC-9 cells apoptosis compared with the control group (Figure 3B). Further, we examined cleaved caspase-3 expression in HCC827 and PC-9 cells with LOC105376794 downregulation by western blotting. The cleaved caspase-3 was obviously decreased in HCC827 and PC-9 cells with LOC105376794 downregulation contrasting to the control group (Figure 3C). In contrast, the pro-caspase-3 expression was obviously increased in HCC827 and PC-9 cells with LOC105376794 downregulation (Figure 3D).

Knockdown of LOC105376794 facilitates the migration and invasion of HCC827 and PC-9 cells. We used Transwell and wound-healing assays to examine the effect of LOC105376794 on cell motility. Compared with the control group, the invasion and migration abilities of cells transfected with sh-LOC105376794 were significantly increased (Figures 4A, 4B). These results indicated that the knockdown of LOC105376794 promoted the invasion and migration of HCC827 and PC-9 cells.

The low expression of LOC105376794 reduces gefitinib sensitivity in HCC827 and PC-9 cells. At first, we explored the gefitinib sensitivities of HCC827 (EGFR 19del), PC-9 (EGFR 19del), and H1975 (EGFR 21L858R mutation) cells. Cell apoptosis assay suggested that the sensitivity of HCC827 and PC-9 cells to gefitinib was better than that of H1975 cells (Figures 5A, 5B). To study the effect of LOC105376794 on the sensitivity of gefitinib, gefitinib-sensitive cell lines (HCC-827 and PC-9) were used. We then investigated the effect of LOC105376794 on apoptosis in HCC827 and PC-9 cells. The results indicated that the apoptosis rate in PC-9 cells almost had no change after LOC105376794 decreased compared with the PC-9 blank group (Figure 5A). The apoptosis rate in HCC827 cells was reduced after LOC105376794 decreased compared with the HCC827-blank group (Figure 5B). Subsequently, we evaluated the effects of LOC105376794 on the gefitinib sensitivity in HCC827 and PC-9 cell lines. Compared with the PC-9/gefitinib group, the knockdown of LOC105376794 suppressed cell apoptosis in the PC-9/sh-LOC105376794/gefitinib group (Figure 5A). We have come to the same conclusion of gefitinib sensitivity in the study of HCC827 cells (Figure 5B). The result illustrated that low expression of LOC105376794 could obviously inhibit the sensitivity of HCC827 and PC-9 cells to gefitinib.

Table 2. The expression of LOC105376794 by sex and smoking stratification in all the patients.

	LOC105376794 expression ($2^{-\Delta ct}$)	p-value
Sex		0.48
male	0.19±0.26	
female	0.11±0.15	
Smoking status		0.21
never smoker	0.13±0.20	
ever smoker	0.19±0.21	

Knockdown of LOC105376794 suppresses the ATF4/CHOP signaling pathway and facilitates the expression of ERK phosphorylation. As mentioned above, the cleaved caspase-3 was obviously decreased in HCC827 and PC-9 cells with LOC105376794 downregulation contrasting to the control group (Figure 3C). GO Term analysis of differentially expressed lncRNAs was carried out to explore the downstream regulatory mechanism by which LOC105376794

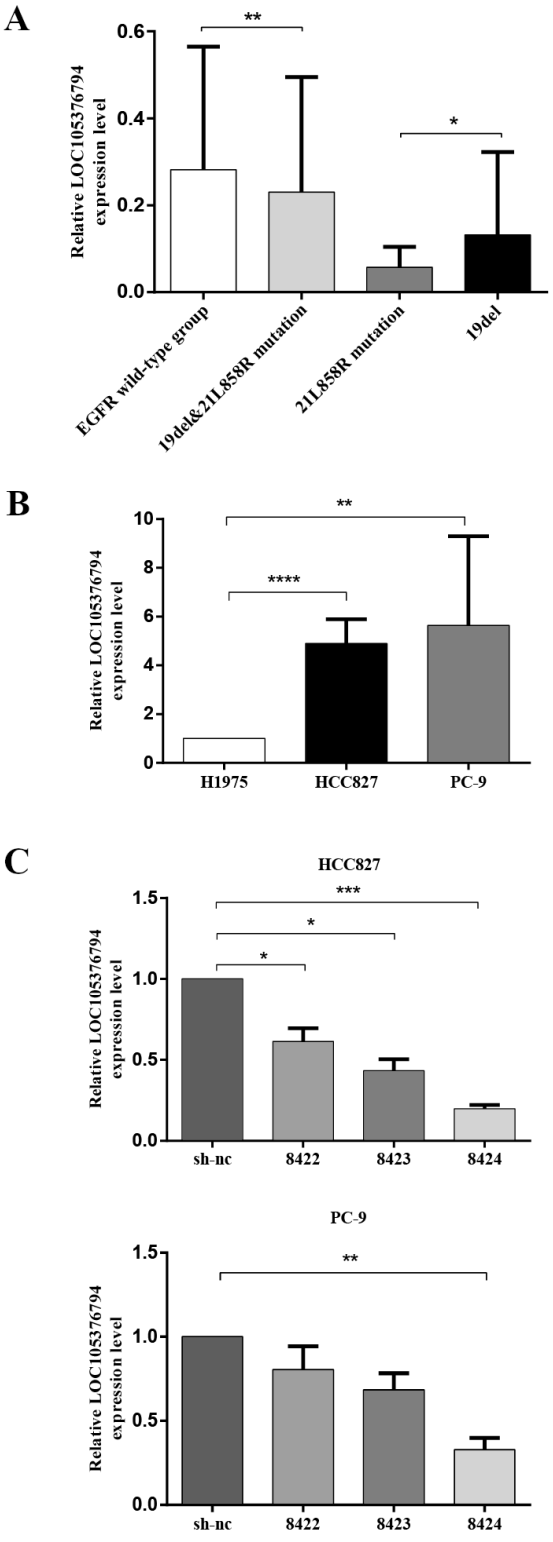

Figure 2. LOC105376794 was highly expressed in the EGFR 19del group. A) Expressions of LOC105376794 were examined in serum by qRT-PCR. B) Expressions of LOC105376794 were examined in HCC827, PC-9, and H1975 cells. C) Knockdown efficiency of LOC105376794 was detected in cells by qRT-PCR. *p<0.05, **p<0.01, ***p<0.001, ****p<0.0001

played a role in HCC827 and PC-9 cells. It was indicated that LOC105376794 regulated the expression of extracellular signal-regulated kinase 1/2 (ERK) phosphorylation expression. Western blot results in Figures 6A–6C showed that the knockdown of LOC105376794 had no influence on the expression level of ERK protein, but obviously increased the expression of ERK phosphorylation in HCC827 and PC-9 cells. The Activating Transcription Factor 4 (ATF4)/C/EBP homologous protein (CHOP) pathway is widely involved in tumor progression [17]. We found that the knockdown of LOC105376794 obviously reduced the expression of ATF4 and CHOP in HCC827 and PC-9 cells (Figures 6A–6C).

Discussion

EGFR-TKIs are the conventional first-line treatment for 19del and 21L858R mutation in LUAD. Patients in the 19del group presented with a better prognosis compared to the 21L858R mutation group under the same treatment regimen. LUAD patients with 19del developed resistance to EGFR-TKIs, leading to the main cause of therapeutic failure. Whether the evolution of LUAD patients with 19del is accompanied by aberrant expression of genes or abnormal regulation currently remains elusive. Therefore, understanding the mechanisms of the development and the EGFR-TKIs sensitivity in LUAD cells with 19del will contribute to enhancing clinical prognosis and reducing EGFR-TKIs resistance. The roles and molecular mechanisms of lncRNAs in LUAD patients with 19del remain unclear. This study intended to discuss the functions of lncRNA LOC105376794 in LUAD cells with 19del. We detected LOC105376794 was significantly upregulated in serum and cell lines with 19del, indicating LOC105376794 was relevant to the progression of LUAD with 19del. We subsequently proved that blocking LOC105376794 effectively regulated cell biofunction and reduced the sensitivity to gefitinib.

A total of 64 differentially expressed lncRNAs interaction with mRNAs and miRNAs between EGFR 19del and 21L858R mutation were identified in serum RNA sequencing. There were 54 lncRNAs evidently interacting with mRNAs in network analysis and 10 lncRNAs related to mRNAs in positional analysis. We found that the expression levels of LOC105376794 showed the same tendency in serum and cells in LUAD. LOC105376794 is expressed in many normal tissues and combines with a variety of promoters and enhancers to mediate target genes. Transcriptome sequencing indicated that URS00009C3FCF (symbol: ENSG00000271732, Location (hg38): chr1:16,607,309-16,626,815) was the transcript of LOC105376794, which was studied in our experiment. Jiang et al. reported that the expression of ENSG00000271732 in LUAD extracellular vesicles was significantly increased. ENSG00000271732 in extracellular vesicles accelerated paracrine secretion of HGF through binding with AUF1, promoted proliferation, invasion, migration, and liver metastasis of LUAD cells

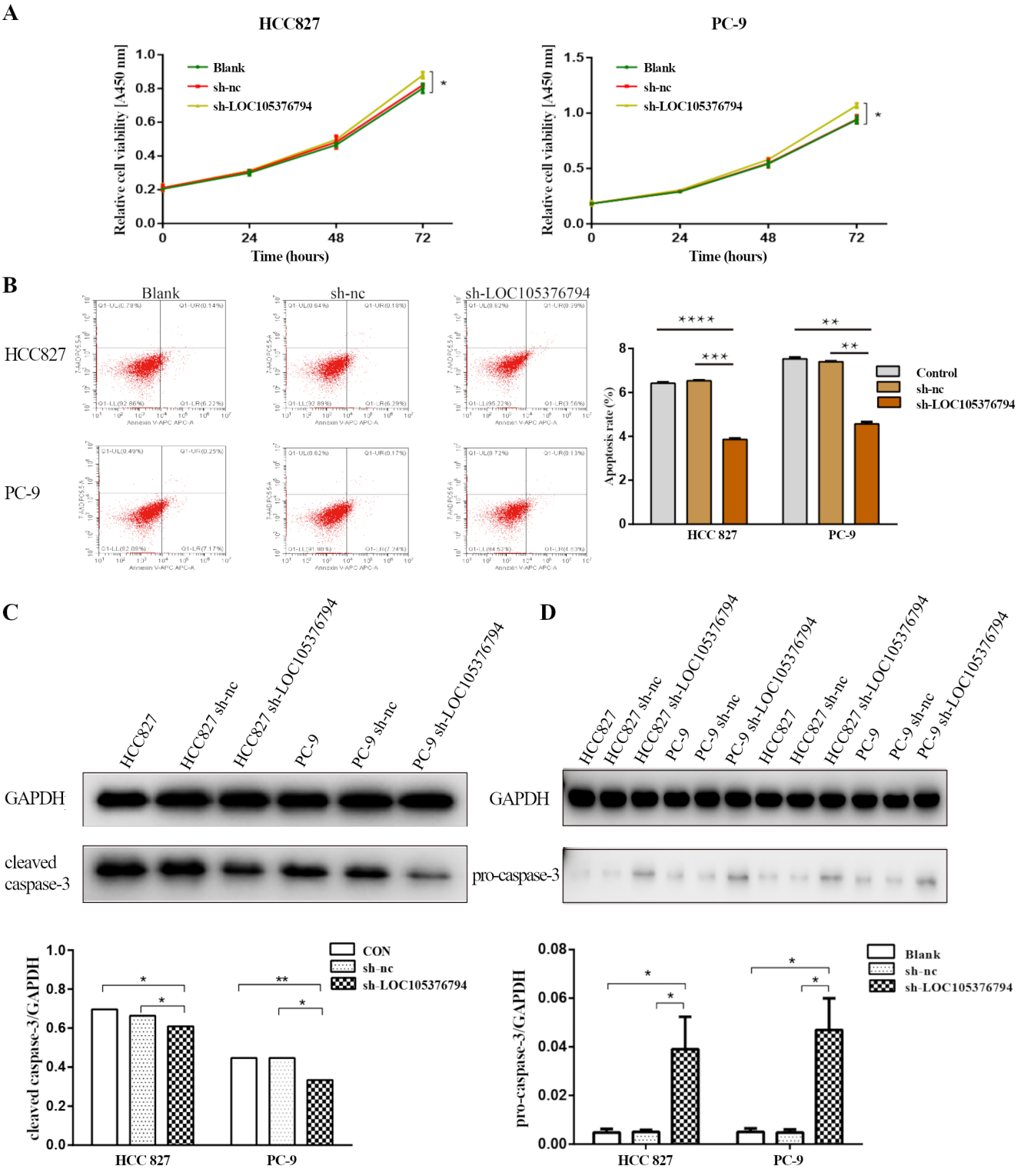

Figure 3. Inhibition of LOC105376794 promoted proliferation and reduced apoptosis of HCC827 and PC-9 cells. A) The proliferation of HCC827 and PC-9 cells was increased by the knockdown of LOC105376794 after 72 h. B) Compared with the control group, the reduction of LOC105376794 expression suppressed apoptosis in HCC827 and PC-9 cells. C) The amount of cleaved caspase-3 was decreased in both HCC827 and PC-9 cells with reduced LOC105376794 expression in contrast to pro-caspase-3 level (D), where the increased expression was observed. *p<0.05, **p<0.01, ***p<0.001, ****p<0.0001

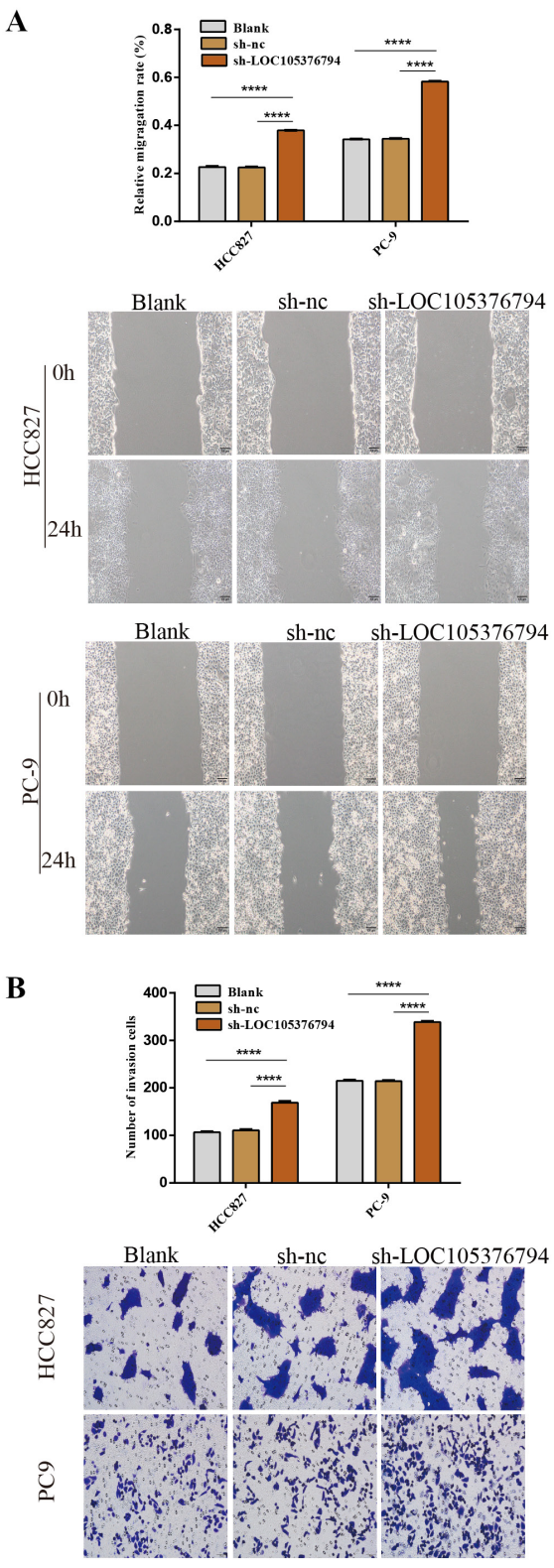

Figure 4. Knockdown of LOC105376794 facilitated the migration and invasion of HCC827 and PC-9 cells. Compared with the control group, the migration (A) and invasion (B) abilities of cells transfected with sh-LOC105376794 were significantly increased. ****p<0.0001

[18]. lncRNAs by functioning as vital factors participated in the regulation of the carcinogenesis process. Zhao et al. identified 41 differentially expressed lncRNAs regulated by tumor protein p53-R273H in cancer stem cells of colorectal cancer and demonstrated that depletion of two lncRNAs, lnc273-31 and lnc273-34, resulted in weakened cancer stem cell self-renewal, invasion, migration, and chemoresistance [19]. Previously, a study by Papaioannou et al. identified that HOXB cluster antisense RNA 3 (HOXB-AS3) interacted with ErbB3-binding protein 1 (EBP1), facilitated EBP1 to ribosomal DNA, and via regulation of ribosomal RNA transcription and protein synthesis radically affected proliferation in acute myeloid leukemia [20]. Circulating lncRNAs could essentially be used as biomarkers to identify the EGFR mutation status, as well as the effect of EGFR-TKI. Lv et al. identified a total of 61 differential lncRNAs between the EGFR mutation group and the wild-type group [21]. A combination of three lncRNAs, Cajal body-specific RNA 7, metastasis-associated lung adenocarcinoma transcript 1, and NONHSAT017369, could precisely distinguish an EGFR mutation from EGFR wild type [21]. An existing study elicited the significance of plasma metastasis-associated lung adenocarcinoma transcript 1 in predicting the efficacy of EGFR-TKIs in non-small cell lung cancer [21]. The relationships between lncRNAs and EGFR mutation status, as well as the biological characteristics between two mutation subtypes, warrant extensive investigation.

ERK and ERK phosphorylation, members of the mitogen-activated protein kinase family, promote fundamental cellular processes such as proliferation, migration and metastasis, and inhibit cell apoptosis of cancer cells [22–25]. The results verified that there was little change in the expression of ERK after the expression of LOC105376794 was reduced, while ERK phosphorylation was altered significantly. LOC105376794 was related to many transcription factors, such as Transcription factor Sp1, Retinoblastoma-associated protein, Transcription factor SOX-5 [26]. These transcription factors regulated the expression of ERK phosphorylation *in vitro* and *in vivo* [27–29]. LOC105376794 might have an influence on ERK phosphorylation via the interaction with transcription factors. Our results demonstrated that it was the ERK signaling pathway, or more precisely the functional ERK phosphorylation caused by inhibition of LOC105376794 may promote the malignant properties of HCC827 and PC-9 cells.

The ATF4/CHOP route has been more widely explored and it plays a crucial role in executing ER stress-induced apoptosis in tumor progression [30]. ATF4 is a transcriptional activator that promotes the expression of a wide range of genes implicated in the enhancement of cell recovery and adaptation to stress conditions [31]. Under prolonged ER stress conditions, ATF4 promotes the expression of transcription factors such as CHOP [32]. It has been repeatedly suggested that CHOP gene expression was strictly involved in cell death by apoptosis [17], promoted

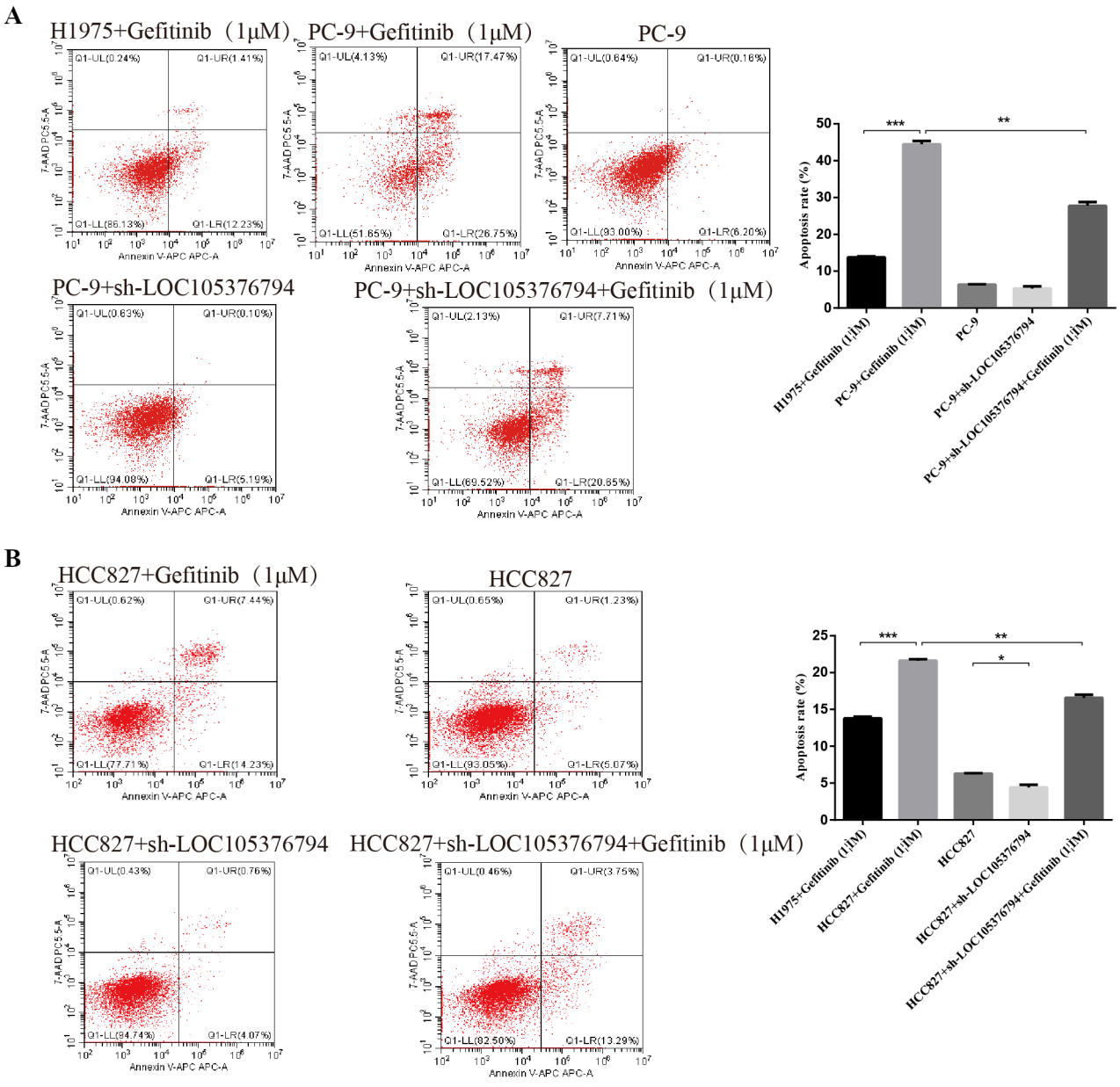

Figure 5. The low expression of LOC105376794 reduced gefitinib sensitivity in PC-9 and HCC827 cells. The sensitivity of HCC827 and PC-9 cells to gefitinib was better than that of H1975 cells. The apoptosis rate in PC-9 cells almost had no change after LOC105376794 decreased compared with the PC-9 blank group. The apoptosis rate in HCC827 cells was reduced after LOC105376794 decreased compared with the HCC827-blank group. Compared with the PC-9/gefitinib group, the knockdown of LOC105376794 suppressed cell apoptosis in the PC-9/sh-LOC105376794/gefitinib group. The same conclusion on gefitinib sensitivity was observed in HCC827 cells. **p<0.01, ***p<0.001

a hyperoxidizing environment causing cell apoptosis [33]. There are some transcription factors binding sites for LOC105376794, for example, KLF6, ATF3. Liu et al. reported that ATF3 and ATF4 are parts of the ATF/cAMP response element binding family [32]. Weng et al. verified that ATF3 could promote the transcription of CHOP and induce apoptosis of tumor cells [34]. Tian et al. found that KLF6 could lead to endoplasmic reticulum stress under UV exposure, inhibit the bound of immunoglobulin binding protein to protein kinase R-like ER kinase, thereby improving the ATF4 mRNA translation [35]. We considered that the low expression of LOC105376794 suppressed the ATF4/CHOP signaling pathway by bonding to KLF6 and ATF3 transcription factors, further reduced apoptosis of HCC827 and PC-9 cells, and impacted the gefitinib sensitivity in PC-9 cells.

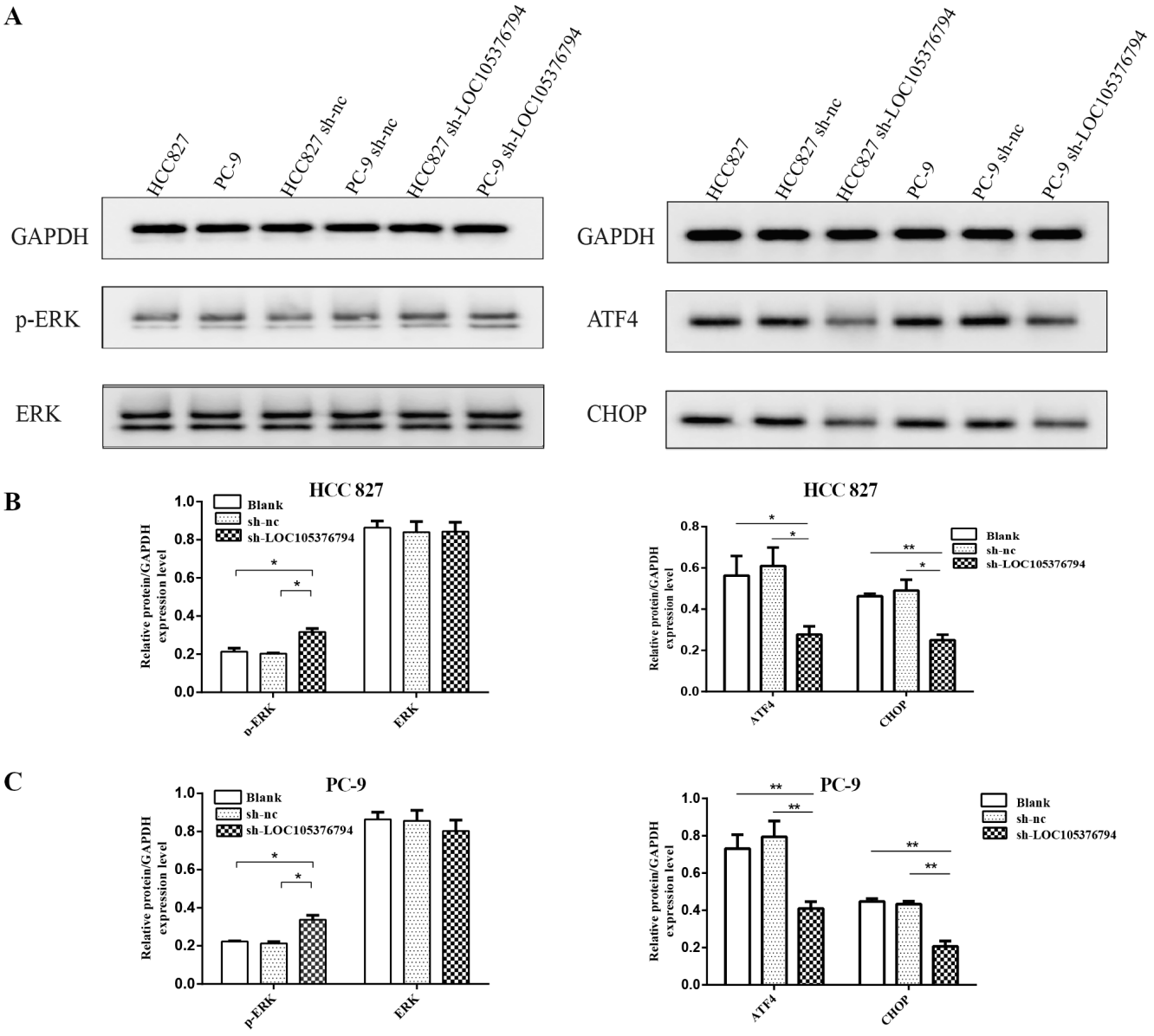

Figure 6. Knockdown of LOC105376794 suppressed cleaved caspase-3 expression, ATF4/CHOP pathway, and facilitated ERK phosphorylation expression. A) The protein of cleaved caspase-3 expression was obviously decreased in HCC827 and PC-9 cells with LOC105376794 downregulation contrasting to the control group. B) Western Blot was used to detect the relative expression levels of p-ERK, ERK, ATF4, and CHOP. C) The expression levels of p-ERK, ERK, ATF4, and CHOP with LOC105376794 decreased in HCC827 and PC-9 cells. All experiments were repeated three times. *p<0.05, **p<0.01

LOC105376794 altered the cell biological behavior and gefitinib sensitivity of LUAD cells with EGFR 19del through the ATF4/CHOP signaling pathway and the expression of ERK phosphorylation. Our results further illustrated the fact that LUAD patients with 19del presented with a more favorable clinical outcome and provided a theoretical basis for treatment strategy for LUAD patients with 19del.

Supplementary information is are available in the online version of the paper.

Acknowledgments: We thank Fule Translation Co., Ltd., Tangshan, China for editing this manuscript. This work was supported by a grant from the Natural Science Foundation of Liaoning Province (2020-ZLLH-43) and the Science and Technology Program of Shenyang, Liaoning Province (22-321-33-51).

References

[1] SHI Y, AU JS, THONGPRASERT S, SRINIVASAN S, TSAI CM et al. A prospective, molecular epidemiology study of EGFR mutations in Asian patients with advanced non-small-cell lung cancer of adenocarcinoma histology (PIONEER). J Thorac Oncol 2014; 9: 154–162. https://doi.org/10.1097/jto.0000000000000033

[2] HONG W, WU Q, ZHANG J, ZHOU Y. Prognostic value of EGFR 19-del and 21-L858R mutations in patients with non-small cell lung cancer. Oncol Lett 2019; 18: 3887–3895. https://doi.org/10.3892/ol.2019.10715

[3] SHARMA N, GRAZIANO S. Overview of the LUX-Lung clinical trial program of afatinib for non-small cell lung cancer. Cancer Treat Rev 2018; 69: 143–151. https://doi.org/10.1016/j.ctrv.2018.06.018

[4] SCHULER M, PAZ-ARES L, SEQUIST LV, HIRSH V, LEE KH et al. First-line afatinib for advanced EGFRm+ NSCLC: Analysis of long-term responders in the LUX-Lung 3, 6, and 7 trials. Lung Cancer 2019; 133: 10–19. https://doi.org/10.1016/j.lungcan.2019.04.006

[5] EIDE IJZ, HELLAND Å, EKMAN S, MELLEMGAARD A, HANSEN KH et al. Osimertinib in T790M-positive and -negative patients with EGFR-mutated advanced non-small cell lung cancer (the TREM-study). Lung Cancer 2020; 143: 27–35. https://doi.org/10.1016/j.lungcan.2020.03.009

[6] CHEN YR, FU YN, LIN CH, YANG ST, HU SF et al. Distinctive activation patterns in constitutively active and gefitinib-sensitive EGFR mutants. Oncogene 2006; 25: 1205–1215. https://doi.org/10.1038/sj.onc.1209159

[7] YU JY, YU SF, WANG SH, BAI H, ZHAO J et al. Clinical outcomes of EGFR-TKI treatment and genetic heterogeneity in lung adenocarcinoma patients with EGFR mutations on exons 19 and 21. Chin J Cancer 2016; 35: 30. https://doi.org/10.1186/s40880-016-0086-2

[8] ZHU JQ, ZHONG WZ, ZHANG GC, LI R, ZHANG XC et al. Better survival with EGFR exon 19 than exon 21 mutations in gefitinib-treated non-small cell lung cancer patients is due to differential inhibition of downstream signals. Cancer Lett 2008; 265: 307–317. https://doi.org/10.1016/j.canlet.2008.02.064

[9] YUN CH, BOGGON TJ, LI Y, WOO MS, GREULICH H et al. Structures of lung cancer-derived EGFR mutants and inhibitor complexes: mechanism of activation and insights into differential inhibitor sensitivity. Cancer Cell 2007; 11: 217–227. https://doi.org/10.1016/j.ccr.2006.12.017

[10] HASTINGS K, YU HA, WEI W, SANCHEZ-VEGA F, DEVEAUX M et al. EGFR mutation subtypes and response to immune checkpoint blockade treatment in non-small-cell lung cancer. Ann Oncol 2019; 30: 1311–1320. https://doi.org/10.1093/annonc/mdz141

[11] OFFIN M, RIZVI H, TENET M, NI A, SANCHEZ-VEGA F et al. Tumor Mutation Burden and Efficacy of EGFR-Tyrosine Kinase Inhibitors in Patients with EGFR-Mutant Lung Cancers. Clin Cancer Res 2019; 25: 1063–1069. https://doi.org/10.1158/1078-0432.ccr-18-1102

[12] HATA A, YOSHIOKA H, FUJITA S, KUNIMASA K, KAJI R et al. Complex mutations in the epidermal growth factor receptor gene in non-small cell lung cancer. J Thorac Oncol 2010; 5: 1524–1528. https://doi.org/10.1097/JTO.0b013e3181e8b3c5

[13] HONG S, GAO F, FU S, WANG Y, FANG W et al. Concomitant Genetic Alterations With Response to Treatment and Epidermal Growth Factor Receptor Tyrosine Kinase Inhibitors in Patients With EGFR-Mutant Advanced Non-Small Cell Lung Cancer. JAMA Oncol 2018; 4: 739–742. https://doi.org/10.1001/jamaoncol.2018.0049

[14] OZSOLAK F, MILOS PM. RNA sequencing: advances, challenges and opportunities. Nat Rev Genet 2011; 12: 87–98. https://doi.org/10.1038/nrg2934

[15] PENG Y, HUANG X, WANG H. lncRNA ACTA2-AS1 predicts malignancy and poor prognosis of triple-negative breast cancer and regulates tumor progression via modulating miR-532-5p. BMC Mol Cell Biol 2022; 23: 34. https://doi.org/10.1186/s12860-022-00432-7

[16] LI Z. Overexpression of lncRNA HOXA-AS2 promotes the progression of oral squamous cell carcinoma by mediating SNX5 expression. BMC Mol Cell Biol 2022; 23: 59. https://doi.org/10.1186/s12860-022-00457-y

[17] ROZPEDEK W, PYTEL D, MUCHA B, LESZCZYNSKA H, DIEHL JA et al. The Role of the PERK/eIF2α/ATF4/CHOP Signaling Pathway in Tumor Progression During Endoplasmic Reticulum Stress. Curr Mol Med 2016; 16: 533–544. https://doi.org/10.2174/1566524016666160523143937

[18] JIANG C, LI X, SUN B, ZHANG N, LI J et al. Extracellular vesicles promotes liver metastasis of lung cancer by ALAHM increasing hepatocellular secretion of HGF. iScience 2022; 25: 103984. https://doi: 10.1016/j.isci.2022.103984

[19] ZHAO Y, LI Y, SHENG J, WU F, LI K et al. P53-R273H mutation enhances colorectal cancer stemness through regulating specific lncRNAs. J Exp Clin Cancer Res 2019; 38: 379. https://doi.org/10.1186/s13046-019-1375-9

[20] PAPAIOANNOU D, PETRI A. The long non-coding RNA HOXB-AS3 regulates ribosomal RNA transcription in NPM1-mutated acute myeloid leukemia. Nat Commun 2019; 10: 5351. https://doi.org/10.1038/s41467-019-13259-2

[21] LV P, YANG S, LIU W, QIN H, TANG X et al. Circulating plasma lncRNAs as novel markers of EGFR mutation status and monitors of epidermal growth factor receptor-tyrosine kinase inhibitor therapy. Thorac Cancer 2020; 11: 29–40. https://doi.org/10.1111/1759-7714.13216

[22] ZHANG H, LIU J, DANG Q, WANG X, CHEN J et al. Ribosomal protein RPL5 regulates colon cancer cell proliferation and migration through MAPK/ERK signaling pathway. BMC Mol Cell Biol 2022; 23: 48. https://doi.org/10.1186/s12860-022-00448-z

[23] ALBAYRAK G, KORKMAZ FD. Alzheimer's drug Memantine inhibits metastasis and p-Erk protein expression on 4T1 breast cancer cells. Bratisl Lek Listy 2020; 121: 499–503. https://doi.org/10.4149/bll_2020_082

[24] ZHENG HY, SHEN FJ, TONG YQ, LI Y. PP2A Inhibits Cervical Cancer Cell Migration by Dephosphorylation of p-JNK, p-p38 and the p-ERK/MAPK Signaling Pathway. Curr Med Sci 2018; 38: 115–123. https://doi.org/10.1007/s11596-018-1854-9

[25] FAN J, REN D, WANG J, LIU X, ZHANG H et al. Bruceine D induces lung cancer cell apoptosis and autophagy via the ROS/MAPK signaling pathway in vitro and in vivo. Cell Death Dis 2020; 11: 126. https://doi.org/10.1038/s41419-020-2317-3

[26] STELZER G, ROSEN N, PLASCHKES I, ZIMMERMAN S, TWIK M et al. The GeneCards Suite: From Gene Data Mining to Disease Genome Sequence Analyses. Curr Protoc Bioinformatics 2016; 54: 1.30.31–31.30.33. https://doi.org/10.1002/cpbi.5

[27] PARK JS, JUNG IA, CHOI HS, KIM DH, CHOI HI et al. Anti-fibrotic effect of 6-bromo-indirubin-3'-oxime (6-BIO) via regulation of activator protein-1 (AP-1) and specificity protein-1 (SP-1) transcription factors in kidney cells. Biomed Pharmacother 2022; 145: 112402. https://doi.org/10.1016/j.biopha.2021.112402

[28] YANG G, LI J, PENG Y, SHEN B, LI Y et al. Ginsenoside Rb1 attenuates methamphetamine (METH)-induced neurotoxicity through the NR2B/ERK/CREB/BDNF signalings in vitro and in vivo models. J Ginseng Res 2022; 46: 426–434. https://doi.org/10.1016/j.jgr.2021.07.005

[29] VINYALS A, FERRERES JR, CALBET-LLOPART N, RAMOS R, TELL-MARTÍ G et al. Oncogenic properties via MAPK signaling of the SOX5-RAF1 fusion gene identified in a wild-type NRAS/BRAF giant congenital nevus. Pigment Cell Melanoma Res 2022; 35: 450–460. https://doi.org/10.1111/pcmr.13044

[30] MA B, ZHANG H, WANG Y, ZHAO A, ZHU Z et al. Corosolic acid, a natural triterpenoid, induces ER stress-dependent apoptosis in human castration resistant prostate cancer cells via activation of IRE-1/JNK, PERK/CHOP and TRIB3. J Exp Clin Cancer Res 2018; 37: 210. https://doi.org/10.1186/s13046-018-0889-x

[31] HE F, ZHANG P, LIU J, WANG R, KAUFMAN RJ et al. ATF4 suppresses hepatocarcinogenesis by inducing SLC7A11 (xCT) to block stress-related ferroptosis. J Hepatol 2023; 79: 362–377. https://doi.org/10.1016/j.jhep.2023.03.016

[32] LIU Z, SHI Q, SONG X, WANG Y, WANG Y et al. Activating Transcription Factor 4 (ATF4)-ATF3-C/EBP Homologous Protein (CHOP) Cascade Shows an Essential Role in the ER Stress-Induced Sensitization of Tetrachlorobenzoquinone-Challenged PC12 Cells to ROS-Mediated Apoptosis via Death Receptor 5 (DR5) Signaling. Chem Res Toxicol 2016; 29: 1510–1518. https://doi.org/10.1021/acs.chemrestox.6b00181

[33] SIMMEN T, LYNES EM, GESSON K, THOMAS G. Oxidative protein folding in the endoplasmic reticulum: tight links to the mitochondria-associated membrane (MAM). Biochim Biophys Acta 2010; 1798: 1465–1473. https://doi.org/10.1016/j.bbamem.2010.04.009

[34] WENG S, ZHOU L, DENG Q, WANG J, YU Y et al. Niclosamide induced cell apoptosis via upregulation of ATF3 and activation of PERK in Hepatocellular carcinoma cells. BMC Gastroenterol 2016; 16: 25. https://doi.org/10.1186/s12876-016-0442-3

[35] TIAN F, ZHAO J, BU S, TENG H, YANG J et al. KLF6 Induces Apoptosis in Human Lens Epithelial Cells Through the ATF4-ATF3-CHOP Axis. Drug Des Devel Ther 2020; 14: 1041–1055. https://doi.org/10.2147/dddt.S218467

https://doi.org/10.4149/neo_2024_230616N316

Silencing of lncRNA LOC105376794 promotes migration, invasion, and gefitinib resistance of lung adenocarcinoma cells with EGFR 19del mutation by ATF4/CHOP axis and ERK phosphorylation

Wenjing LIU[1], Zhipeng DUAN[2], Yefeng WU[3], Rui MA[1,*]

Supplementary Information

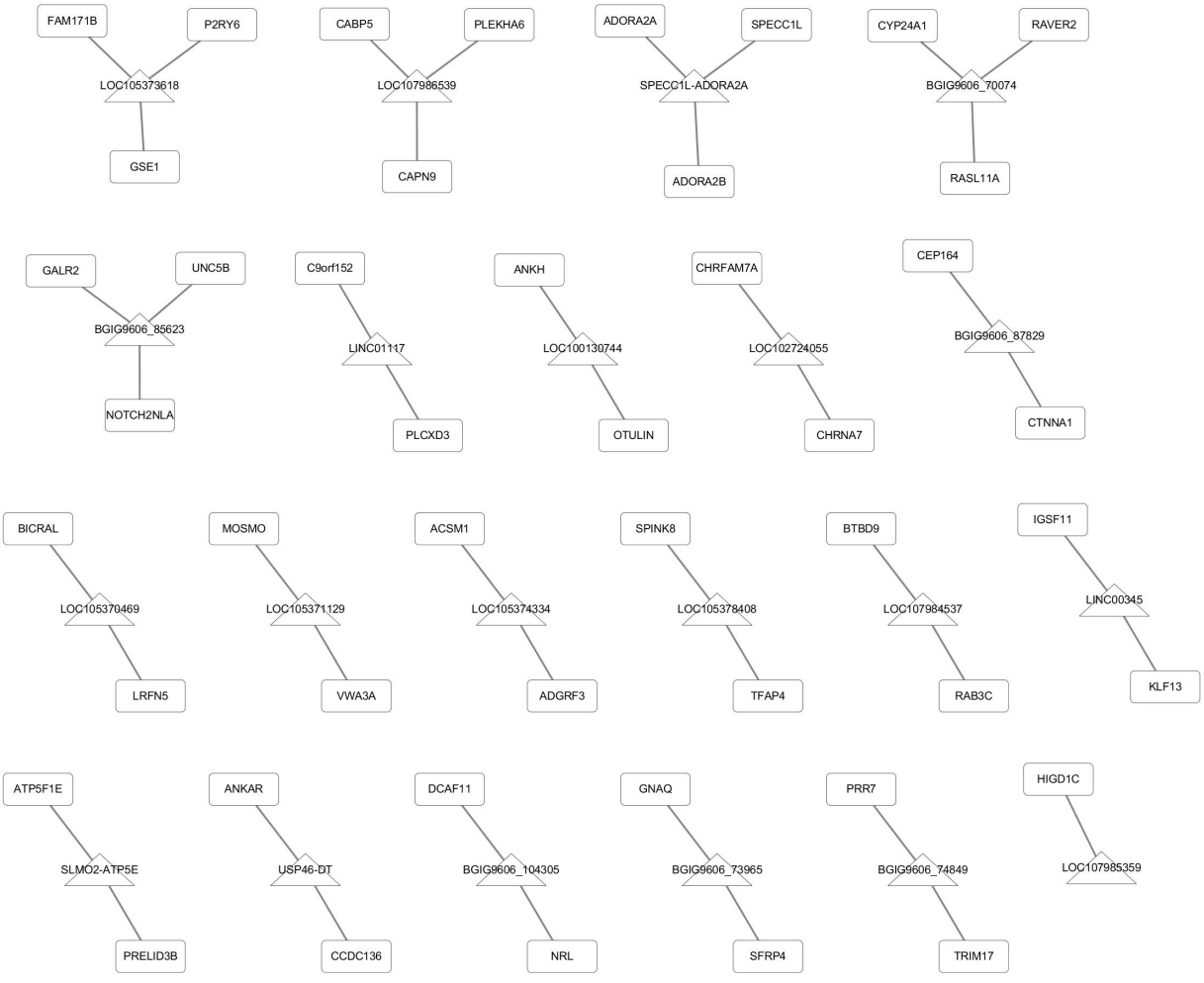

Supplementary Figure S1. The lncRNAs upregulated in 19del group interacted with no more than 3 mRNAs. There were 21 lncRNAs upregulated in 19del group interacted with no more than 3 mRNAs. The triangles mean lncRNAs upregulated in 19del group, the rectangles mean the interacting mRNAs. These mRNAs were DCAF11, NRL, CYP24A1, RASL11A, RAVER2, GNAQ, SFRP4, PRR7, TRIM17, GALR2, NOTCH2NLA, UNC5B, CEP164, CTNNA1, IGSF11, KLF13, C9orf152, PLCXD3, ANKH, OTULIN, CHRFAM7A, CHRNA7, BICRAL, LRFN5, MOSMO, VWA3A, FAM171B, GSE1, P2RY6, ACSM1, ADGRF3, SPINK8, TFAP4, BTBD9, RAB3C, ATP5F1E, PRELID3B, ADORA2A, ADORA2B, SPECC1L, ANKAR, CCDC136.

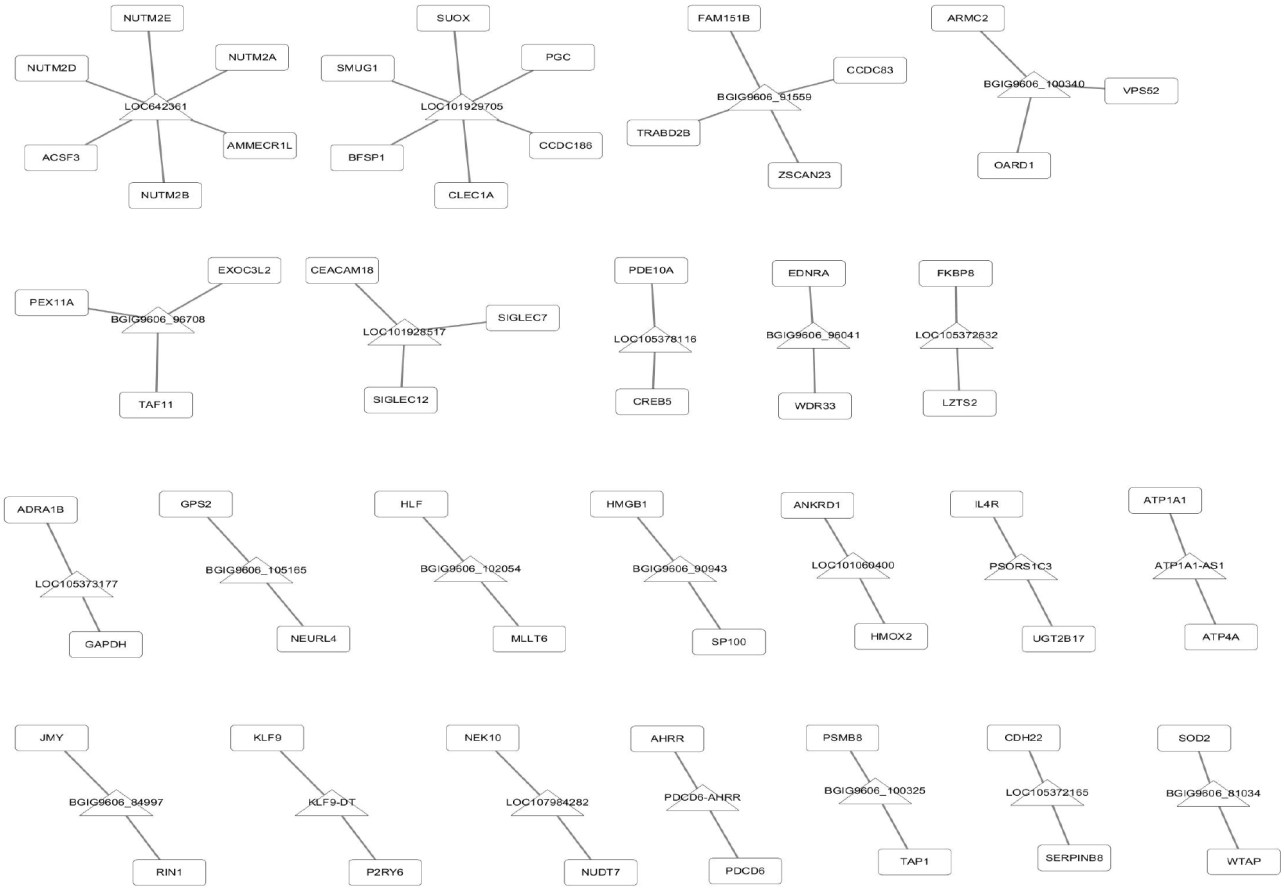

Supplementary Figure S2. The lncRNAs upregulated in 21L858R mutation group interacted with mRNAs in network analysis. There were 23 lncRNAs were upregulated in 21L858R mutation, interacting with 59 mRNAs. The mRNAs were ATP1A1, ATP4A, PSMB8, TAP1, ARMC2, OARD1, VPS52, HLF, MLLT6, GPS2, NEURL4, SOD2, WTAP, JMY, RIN1, HMGB1, SP100, CCDC83, FAM151B, TRABD2B, ZSCAN23, EDNRA, WDR33, PEX11A, TAF11, EXOC3L2, KLF9, P2RY6, ANKRD1, HMOX2, CEACAM18, SIGLEC12, SIGLEC7, BFSP1, CCDC186, CLEC1A, PGC, SMUG1, SUOX, CDH22, SERPINB8, FKBP8, LZTS2, ADRA1B, GAPDH, CREB5, PDE10A, NEK10, NUDT7, ACSF3, AMMECR1L, NUTM2A, NUTM2B, NUTM2D, NUTM2E, AHRR, PDCD6, IL4R, UGT2B17.

Supplementary Table S1. Differentially expressed lncRNAs evidently interacted with mRNAs.

lncRNAs upregulated in 19del group		lncRNAs upregulated in L858R mutation group	
lncRNAs	**log2 (E21L858R/E19Del)**	**lncRNAs**	**log2 (E21L858R/E19Del)**
LOC105374334	–25.17240242	LOC101928517	22.70446555
LOC105378375	–24.71548577	BGIG9606_100340	22.55436589
BGIG9606_85623	–24.28606858	PDCD6-AHRR	22.48932665
BGIG9606_87829	–24.19619831	BGIG9606_100325	22.44673369
SAP30-DT	–23.40778846	BGIG9606_81034	22.40131901
LINC00345	–23.30346304	LOC105372165	21.90759527
SLMO2-ATP5E	–23.20851837	ATP1A1-AS1	21.8561111
BGIG9606_104305	–23.19286571	LOC107984282	21.75168112
BGIG9606_74849	–23.19286571	LOC105378116	21.41261551
LOC107986539	–23.16436627	BGIG9606_96041	21.41066807
BGIG9606_70074	–22.93988193	LOC101060400	21.28303378
LOC105370469	–22.66013627	KLF9-DT	21.03702033
BGIG9606_88096	–22.59760662	BGIG9606_96708	20.98495159
ANAPC1P4	–22.56952039	BGIG9606_105165	20.8632532
LOC100130744	–22.48377692	BGIG9606_102054	20.80992115
LOC102724055	–22.47654596	BGIG9606_84997	20.53672365
BGIG9606_104089	–21.54960251	BGIG9606_91559	20.4902537
SPRR2C	–21.50044056	BGIG9606_90943	20.46486442
LINC01117	–21.4333131	LOC105372632	20.44170734
LOC105374535	–10.63797098	PSORS1C3	8.480839436
LOC105376794	–10.25418507	LOC105373177	8.217013535
LOC107984537	–10.2349723	LOC642361	8.099063852
LOC105371129	–9.968732556	LOC101929705	6.619267203
BGIG9606_82787	–9.835844448		
BGIG9606_73965	–9.373448294		
SPECC1L-ADORA2A	–9.307588977		
LOC105378408	–9.2985423		
USP46-DT	–9.286934826		
LOC152048	–9.204749327		
LOC105373618	–8.87165355		
LOC107985359	–7.882966356		